

1 **Detection of SARS-CoV-2 from raw patient samples by coupled high temperature**  
2 **reverse transcription and amplification**

3 Johannes W. P. Kuiper<sup>1#</sup>, Timo Baade<sup>1,6#</sup>, Marcel Kremer<sup>2</sup>, Ramon Kranaster<sup>3</sup>, Linda  
4 Irmisch<sup>4</sup>, Marcus Schuchmann<sup>4</sup>, Johannes Zander<sup>2</sup>, Andreas Marx<sup>3,5,6</sup>, and Christof R.  
5 Hauck<sup>1,6\*</sup>

6

7 <sup>1</sup>Lehrstuhl Zellbiologie, Universität Konstanz, 78457 Konstanz, Germany

8 <sup>2</sup>Labor Dr. Brunner, Luisenstr. 7e, 78464 Konstanz, Germany

9 <sup>3</sup>myPOLs Biotec GmbH, Blarerstraße 56, 78462 Konstanz, Germany

10 <sup>4</sup>Klinikum Konstanz, Mainaustraße 35, 78464 Konstanz, Germany

11 <sup>5</sup>Lehrstuhl Organische Chemie/Zelluläre Chemie, Universität Konstanz, 78457 Konstanz,  
12 Germany

13 <sup>6</sup>Konstanz Research School Chemical Biology, Universität Konstanz, 78457 Konstanz, Germany

14 # both authors contributed equally

15 \* address correspondence to:

16 Christof R. Hauck

17 Lehrstuhl Zellbiologie

18 Fachbereich Biologie 621

19 Universität Konstanz

20 Universitätsstrasse 10

21 78457 Konstanz

22 phone: +49-(0)7531-88-2286

23 fax: +49-(0)7531-88-4036

24 e-mail: [christof.hauck@uni-konstanz.de](mailto:christof.hauck@uni-konstanz.de)

25 **Abstract**

26 The SARS-CoV-2 beta coronavirus is spreading globally with unprecedented  
27 consequences for modern societies. The early detection of infected individuals is a pre-  
28 requisite for all strategies aiming to contain the virus. Currently, purification of RNA from  
29 patient samples followed by RT-PCR is the gold standard to assess the presence of this  
30 single-strand RNA virus. However, these procedures are time consuming, require  
31 continuous supply of specialized reagents, and are prohibitively expensive in resource-  
32 poor settings. Here, we report an improved nucleic-acid-based approach to detect SARS-  
33 CoV-2, which alleviates the need to purify RNA, reduces handling steps, minimizes costs,  
34 and allows evaluation by non-specialized equipment. The use of unprocessed swap  
35 samples and the ability to detect as little as three viral genome equivalents is enabled by  
36 employing a heat-stable RNA- and DNA-dependent DNA polymerase, which performs the  
37 double task of stringent reverse transcription of RNA at elevated temperatures as well as  
38 PCR amplification of a SARS-CoV-2 specific target gene. As results are obtained within 2  
39 hours and can be read-out by a hand-held LED-screen, this novel protocol will be of  
40 particular importance for large-scale virus surveillance in economically constrained  
41 settings.

42

43

## 44 **Introduction**

45 As of April 2020, severe acute respiratory syndrome coronavirus 2 (SARS-CoV-2) is  
46 responsible for more than 4.1 million COVID-19 cases and associated with more than  
47 285.000 fatalities (WHO; COVID situation report 114 [Accessed 14. May 2020]. Available  
48 from: [https://www.who.int/emergencies/diseases/novel-coronavirus-2019/situation-](https://www.who.int/emergencies/diseases/novel-coronavirus-2019/situation-reports)  
49 [reports](https://www.who.int/emergencies/diseases/novel-coronavirus-2019/situation-reports)). Within a few months of its emergence, this infectious agent has spread globally  
50 and is derailing societies worldwide. SARS-CoV-2 is an enveloped plus-strand RNA virus  
51 of the beta-coronavirus genus with closely related strains circulating in bats and some  
52 other mammals indicating a zoonotic origin (Lu, Zhao et al., 2020, Zhou, Yang et al.,  
53 2020). Upon host cell infection, beta-coronaviruses generate a minus-strand RNA copy of  
54 their genome by a virus-encoded RNA-dependent RNA-polymerase (Snijder, Decroly et  
55 al., 2016). Furthermore, the virus directs the synthesis of several subgenomic minus  
56 strand RNAs, which are complementary to the 3' of the viral genome and which encode  
57 several non-structural proteins including the N gene (Snijder et al., 2016). Therefore,  
58 infected cells harbor plus and minus strand RNAs of the coronavirus, with an  
59 overabundance of transcripts derived from the 3' end of its genome (Den Boon, Spaan et  
60 al., 1995, Nedialkova, Gorbalenya et al., 2010). As with other RNA viruses, confirmation  
61 of SARS-CoV-2 infection is based on the molecular biological detection of the viral  
62 genome and its transcripts in patient samples by nucleic acid amplification techniques  
63 (NAATs) (Zumla, Al-Tawfiq et al., 2014). To allow sensitive and accurate detection of viral  
64 ribonucleic acids, primary patient samples such as nasopharyngeal swabs, sputum or  
65 stool are further processed to isolate the total RNA. Using reverse transcriptase, the RNA  
66 is then reverse transcribed into DNA. Next, the DNA is PCR-amplified by a thermo-stable

67 DNA-dependent DNA polymerase using specific primers and probes to detect the  
68 presence of SARS-CoV-2 sequences.

69 Facilitated by genome sequencing and rapid information sharing, such a NAAT-based  
70 diagnostic surveillance of SARS-CoV-2 has been in place right from the beginning of the  
71 COVID-19 pandemic (Wu, Zhao et al., 2020; Corman, Landt et al., 2020). However, the  
72 current methodology is laborious, requires multiple handling steps and expensive  
73 consumables, resulting in a costly diagnostic procedure, which can constrain COVID-19  
74 testing in economically tight settings. Furthermore, the overwhelming worldwide demand  
75 for some of the same reagents (such as those needed for RNA isolation) and diagnostic  
76 kits has produced shortages and unnecessarily delayed or restricted testing. From a  
77 clinical point of view, rapid testing and early decision making on further isolation measures  
78 for patients and health care workers remains a critical issue.

79 We have developed a thermostable DNA polymerase, which can mediate DNA synthesis  
80 from both RNA as well as DNA templates (Sauter & Marx, 2006). By targeted  
81 modifications, we have further improved the accuracy and processivity of this enzyme  
82 (Blatter, Bergen et al., 2013), which lays the foundation of the commercialized Volcano3G  
83 formulations. We reasoned that such a bi-functional enzyme might allow us to improve  
84 and simplify the detection of RNA viruses. Here we show that Volcano3G can be used in  
85 a coupled high-temperature reverse transcription and amplification reaction to detect  
86 SARS-CoV-2 with high sensitivity and specificity. Moreover, our findings demonstrate the  
87 usefulness of such a thermo-stable RNA- and DNA-reading DNA polymerase to simplify  
88 COVID-19 diagnostics. Most importantly, we can show that this robust enzyme allows  
89 detection of SARS-CoV-2 directly from unprocessed patient material. Accordingly, this  
90 streamlined procedure, which does not depend on limited reagents, nor requires

91 expensive equipment, is poised to enable large scale SARS-CoV-2 surveillance in a  
92 multitude of resource- or time-constrained settings.

93 **Results and Discussion**

94 **A RNA- and DNA-reading heat-stable polymerase reverse transcribes and amplifies**  
95 **viral RNA**

96 Evidence of an acute SARS-CoV-2 infection depends on the detection of viral RNA  
97 species in patient samples, which necessitates reverse transcription of RNA followed by  
98 PCR amplification of the resulting DNA. To investigate, if the Volcano polymerase is able  
99 to perform both of these steps, we employed an *in vitro* transcribed synthetic SARS-CoV-  
100 2 RNA template covering a ~750 nt stretch within the 3'-end of the viral genome (Fig. 1A).  
101 This target region is also included in the CDC panel of primers (Division of Viral Diseases,  
102 National Center for Immunization and Respiratory Diseases, Centers for Disease Control  
103 and Prevention, Atlanta, GA, USA; [https://www.cdc.gov/coronavirus/2019-ncov/lab/rt-pcr-](https://www.cdc.gov/coronavirus/2019-ncov/lab/rt-pcr-panel-primer-probes.html)  
104 [panel-primer-probes.html](https://www.cdc.gov/coronavirus/2019-ncov/lab/rt-pcr-panel-primer-probes.html); accessed on 5.5.2020). When 5000 genome equivalents of the  
105 purified, *in vitro* transcribed viral RNA was used as a PCR template for a generic, heat-  
106 stable DNA-dependent DNA polymerase (Taq DNA polymerase) no amplification  
107 occurred, demonstrating the absence of a contaminating DNA template (Fig. 1B).  
108 However, upon addition of the Volcano3G polymerase to the mix, the expected  
109 amplification product was obtained, confirming that the Volcano3G polymerase can read  
110 the RNA template to produce and amplify a specific DNA sequence (Fig. 1B). Clearly, the  
111 Taq DNA polymerase was able to yield an amplicon, when DNA instead of RNA was used  
112 as a template (Fig. 1B). Not surprisingly, the Volcano3G polymerase was able to operate  
113 with primers and probes supplied by other manufacturers targeting the same region of the  
114 SARS-CoV-2 N gene (Suppl. Fig. S1A and S1B). Due to the thermostability of the  
115 Volcano3G polymerase, this RNA-reading enzyme could perform, in contrast to other  
116 widely used enzymes, the reverse transcription under stringent, high-temperature

117 conditions. Reverse transcription at elevated temperatures could help to overcome stable  
118 RNA-secondary structures present in beta-coronavirus genomes (Brierley, Digard et al.,  
119 1989, Plant, Perez-Alvarado et al., 2005). To take advantage of this particular feature of  
120 the Volcano3G polymerase, we added an extended, high-melting temperature virus-  
121 specific primer (R2) to the reaction, and adjusted the PCR protocol to include a high-  
122 temperature reverse transcription step. As the 3'-end of the viral genomic plus-strand RNA  
123 and its minus-strand complementary sequences are the most abundant nucleic acids in  
124 coronavirus-infected cells, we focussed on the coronavirus N gene, which is located at  
125 the very 3'-end of the SARS-CoV-2 genome (Irigoyen, Firth et al., 2016). Furthermore, the  
126 amino terminus of the N protein varies greatly between different human-pathogenic beta-  
127 coronavirus isolates (Suppl. Fig. S1C), making this region an ideal target for SARS-CoV-  
128 2-specific primers. Accordingly, the high-temperature RT primer R2 was designed to be  
129 complementary to sequences at the 5' end of the N gene (Fig. 1A). The addition of the R2  
130 primer consistently increased the performance of the Volcano3G reaction resulting in  
131 lower cq-values over a wide range of template concentrations (Fig. 1C). The high-  
132 temperature reverse transcription afforded by Volcano3G polymerase and the R2 primer  
133 was optimal at 75°C (Suppl. Fig. S1D). Most importantly, addition of R2 lowered the limit  
134 of detection (LOD) to five copies of the viral genome equivalent (Fig. 1D). To assess, if  
135 this adapted procedure also allows the sensitive detection of SARS-CoV-2 in patient  
136 material, we used RNA isolated from nasopharyngeal swabs of two confirmed COVID-19  
137 cases. In both samples, amplification of the human RNaseP transcript demonstrated the  
138 integrity of the samples and resulted in similar cq-values in the presence or absence of  
139 the additional R2 primer, while the non-template control (NTC) gave no signal (Fig. 1E).  
140 Most importantly, the Volcano3G polymerase detected viral RNA in both samples, but

141 produced exceptionally low cq-values upon addition of the R2 primer, suggesting that the  
142 high-temperature reverse transcription by the thermo-stable RNA-reading DNA  
143 polymerase opens an additional window of opportunity for hypersensitive detection of viral  
144 RNA. Together, these initial results encouraged the further exploration of the Volcano3G  
145 polymerase for facilitating the detection of SARS-CoV-2 RNA.

146  
147 **SARS-CoV-2 detection by high-temperature RT-PCR in a patient cohort delivers**  
148 **results consistent with the standard procedure**

149 To evaluate the potential of the high-temperature RT-PCR protocol using Volcano3G for  
150 the detection of viral RNAs in patient material, we assessed the presence of SARS-CoV-  
151 2 in RNA isolated from a small cohort of COVID-19 suspected cases. RNA was isolated  
152 from nasopharyngeal swabs and the isolated nucleic acid was then evaluated in parallel  
153 by i) a commercial in vitro diagnostic kit (Allplex, Seegene) and ii) high-temperature RT-  
154 PCR with Volcano3G. Of the 43 samples, the Allplex-assay detected the SARS-CoV-2 N  
155 gene in 35 samples, while 8 samples remained negative (Fig. 2A). The eight negative  
156 samples also did not yield amplicons in the Allplex-assay for the RdRp or the E gene (data  
157 not shown). When the 43 RNA samples were employed in high-temperature RT-PCR with  
158 Volcano3G polymerase, the identical results were obtained, showing complete  
159 consistency with regard to positive and negative outcomes (Fig. 2A and 2B). Pairwise  
160 comparison of the cq-values obtained for the isolated RNA samples in detecting the N  
161 gene revealed that the high-temperature RT-PCR with Volcano3G resulted in lower cq-  
162 values throughout all samples suggesting a slightly increased sensitivity (Fig. 2C). In  
163 addition to the resolution of RNA secondary structures, the increased sensitivity might be  
164 due to the fact that the high temperature reverse transcription step involves several cycles,

165 which allow initial highly stringent amplification of viral target genes. Though the high  
166 temperature RT-PCR with Volcano3G was slightly more sensitive, the results correlated  
167 extremely well over a wide range of cq-values with the results obtained by the commercial  
168 assay ( $r^2=0.980$ ,  $p<0.0001$ , Fig. 2D). Together, these findings suggest that high  
169 temperature RT-PCR with Volcano3G could be an additional option to rapidly detect RNA-  
170 virus genomes with high specificity and sensitivity.

171  
172 **High-temperature RT-PCR using Volcano3G polymerase allows SARS-CoV-2**  
173 **detection from unprocessed patient samples**

174 Besides enhanced stringency and possible resolution of RNA secondary structures, we  
175 speculated that high-temperature RT-PCR might promote viral lysis and allow the  
176 detection of SARS-CoV-2 RNA directly from unprocessed patient samples. To this end,  
177 we employed a second cohort of samples, where each nasopharyngeal swab was  
178 initially resolved in 300  $\mu$ l of distilled water. While 150  $\mu$ l of these diluted samples were  
179 used for RNA extraction and standard RT-PCR, 12  $\mu$ l of the diluted sample were directly  
180 employed in high-temperature RT-PCR with the Volcano3G polymerase. Importantly,  
181 even with this raw patient material, the high-temperature RT-PCR yielded clear-cut  
182 results without increasing the background (Fig. 3A). When directly compared to the  
183 results obtained by the standard RT-PCR from purified RNA of the identical samples, all  
184 negative samples were consistent between the two approaches suggesting that there is  
185 no increased risk of producing false positive results when using the unprocessed patient  
186 samples (Fig. 3B). Moreover, 100% of the samples showing cq-values of  $\leq 30$  for the  
187 SARS-CoV-2 N gene in the standard RT-PCR assay with purified RNA were correctly  
188 identified by the Volcano3G high-temperature RT-PCR employing raw patient samples

189 (Fig. 3B). Samples yielding cq-values above 30 in the standard RT-PCR following RNA  
190 extraction, which would represent a low viral load, were only rarely detected as positive,  
191 when patient samples were used without further processing (1 in 5 samples, Fig. 3B).  
192 None of these 5 patients with low viral loads was hospitalized and all of them showed  
193 only mild symptoms including sore throat and rhinitis. It is important to stress that clinical  
194 studies of viral dynamics in patients have shown that SARS-CoV-2 titers in swab  
195 samples are most often high during the initial phase of the infection, even before onset  
196 of symptoms (Pan, Zhang et al., 2020, Zou, Ruan et al., 2020). In contrast, low titers are  
197 typically seen at the later phase of the infection and can even be detected after the  
198 resolution of symptoms (Lescure, Bouadma et al., 2020). If infectious virus is spread in  
199 situations, where viral titers are low, is still unclear.

200 Interestingly, for most positive samples detected by the high-temperature RT-PCR with  
201 Volcano3G, the cq-values were lower compared to the standard RT-PCR (Fig. 3C and  
202 D), indicating that the detection of SARS-CoV-2 from unprocessed patient material might  
203 not be limited by the sensitivity of this direct approach. As unprocessed swab material  
204 might contain numerous patient-derived proteins, mucus, or membrane fragments, we  
205 speculated that substance(s) within these raw samples could interfere and inhibit the  
206 detection of SARS-CoV-2 when only a low viral load is present. Therefore, we tested the  
207 inhibitory potential of the eluted swab material. Using the in vitro transcribed viral RNA  
208 as a template, we spiked the Volcano3G reaction mix with increasing amounts of swab-  
209 derived material (Fig. 3E). Importantly, there was a clear dose-dependent inhibition of  
210 the amplification reaction due to the material eluted from the swabs (Fig. 3E and Suppl.  
211 Fig. S2). The extent of inhibition showed variability between individual samples (Suppl.  
212 Fig. S2), with some samples leading to complete inhibition of viral detection at 10%

213 added swab material (Fig. 3E). Especially, for samples containing low viral titers this  
214 could significantly elevate the LOD. Therefore, we supplemented the distilled water used  
215 for eluting the nasopharyngeal swabs with betaine, BSA, carrier RNA, DTT or treated  
216 them with proteinase K or combinations of these reagents, with the idea that these  
217 substances might be able to alleviate the inhibition due to inhibitory proteins or RNA  
218 degrading or oxidizing agents. Indeed, several of the treatments enhanced the detection  
219 of SARS-CoV-2 from an unprocessed patient sample demonstrating that it is possible to  
220 partially overcome the inhibitory effect of the raw material (Suppl. Fig. 3A and B).  
221 Furthermore, we reasoned that increasing the volume of the high-temperature RT-PCR  
222 reaction to allow an increase of viral copies without increasing the relative abundance of  
223 inhibitory factors could also help in improving the detection of SARS-CoV-2 in low-titer  
224 patient samples. Using addition of carrier RNA and DTT as well as an increased input,  
225 we assayed an additional set of five SARS-CoV-2 positive samples, which had produced  
226 ct values >30 for the N gene in the standard RT-PCR procedure with purified RNA (Fig.  
227 3F). Interestingly, 3 of the 5 samples could now be detected as positive, when the  
228 unprocessed samples were used as input for the high temperature RT-PCR with  
229 Volcano3G polymerase (Fig. 3F). These results demonstrate that even low virus titers  
230 can be detected directly from raw patient samples by employing the high temperature  
231 RT-PCR conditions. Though further improvements will be necessary to consistently  
232 detect SARS-CoV-2 RNA in unprocessed low-titer samples, bypassing the need for RNA  
233 purification dramatically accelerates and simplifies the evaluation of patient material. As  
234 an additional feature, we have observed that the endpoint of the high temperature RT-  
235 PCR with Volcano3G polymerase can also be easily evaluated on a blue-light LED

236 screen, yielding strong green fluorescence for positive samples and allowing clear-cut  
237 differentiation by the naked eye (Fig. 3G).

238 Together, the use of a heat-stable, RNA- and DNA-reading polymerases is poised to  
239 simplify detection of viral RNAs. By reducing handling steps, the chances of sample  
240 cross-contamination are minimized. The overwhelming dynamic spread of SARS-CoV-2  
241 and the apparent bottle-necks in virus testing highlight the need for additional  
242 methodology that can be deployed in resource poor settings and that is operative in  
243 situations, where particular reagents such as RNA isolation kits might become scarce.  
244 Therefore, the direct detection of virus RNA from unprocessed patient samples and the  
245 ability to perform and read out complex NAAT procedures using standard field PCR  
246 machines and blue-light screens could dramatically expand the COVID-19 testing  
247 capabilities and might also afford an important economic relief for health care providers  
248 in large parts of the world.

249

250

## 251 **Material and Methods**

252

### 253 *Patient samples and ethics statement*

254 Nasopharyngeal swabs were collected at the COVID-19 test center hosted at the Klinikum  
255 Konstanz. Samples used in this study were procured with sterile dry swabs (Copan 160C  
256 Rayon, [www.copaninnovation.com](http://www.copaninnovation.com); Eurotubo collection swab 300253, [www.deltalab.es](http://www.deltalab.es);  
257 culture swab without transport medium 09-516-5009, [www.nerbe-plus.de](http://www.nerbe-plus.de)) and samples  
258 were processed within 24h. Patients gave informed consent to participate in the study  
259 “*Entnahme von Schleimhautabstrichen zur Detektion von Sars-CoV-2 bei Verdacht auf*  
260 *COVID-19*” registered at the German Clinical trials Register (DRKS00021578). The study  
261 was approved by the local ethics committee of University of Konstanz (05/2020).

262

### 263 *RNA extraction*

264 Nasopharyngeal swabs were eluted in 350 µl RNase/DNase free deionized water and  
265 150 µl of the eluate was used for RNA isolation using the NucleoSpin 96 RNA kit  
266 (Macherey-Nagel, Düren, Germany), where the RA1 lysis buffer included in the kit was  
267 supplemented with 10 µg/ml of carrier RNA (Qiagen, Hilden, Germany) and 15 mM DTT.  
268 Automated handling of the samples was accomplished using the Integra Assist Plus  
269 pipetting robot (Integra, Biebertal, Germany). Finally, purified RNA was eluted into 60 µl  
270 RNase/DNase free deionized water.

271

### 272 *Generation of in vitro transcribed N1 amplicon*

273 cDNA was generated from isolated viral RNA using the Maxima cDNA synthesis kit  
274 (Fermentas, Vilnius, Lithuania) according to the manufacturer’s protocol. A region

275 corresponding to position 27923-28648 of the SARS-CoV2 genome (NC\_045512.2) was  
 276 amplified with Pfu DNA polymerase (primers Clone\_N1\_F and Clone\_N1\_R, see table 1).  
 277 The resulting 726 bp amplicon was purified, digested (KpnI/BamHI) and ligated in  
 278 pBluescript-KS(+). The resulting plasmid was linearized with BamHI, purified and  
 279 transcribed in vitro (T7 DNA polymerase, NEB) for 4 hours at 37°C to yield a 753 nt  
 280 transcript. The purified transcript was treated with RNase-free DNase (Roche) for 4 hours  
 281 at 37°C and purified again (viral RNA isolation kit, Qiagen).

282

283 **Table 1:** Primer and probe sequences used in this study

284

Molecular cloning		
Oligo name	Sequence	Final concentration
Clone_N1_F	5'-TATAGGTACCCACAACCTGTAGCTGCATTTCCACC-3'	500 nM
Clone_N1_R	5'-TATAGGATCCGATATCAGCACCATAGGGAAGTCCAGC-3'	500 nM
Real time PCR		
Oligo name	Sequence	Final concentration
CDC_N1-F	5'-GACCCCAAATCAGCGAAAT-3'	670 nM
CDC_N1-R	5'-TCTGGTTACTGCCAGTTGAATCTG-3'	670 nM
CDC_N1-P	5'-FAM-ACCCCGCATTACGTTTGGTGGACC-BHQ1-3'	170 nM
RnaseP-F	5'-AGATTTGGACCTGCGAGCG-3'	670 nM
RnaseP-R	5'-GAGCGGCTGTCTCCACAAGT-3'	670 nM
RnaseP-P	5'-FAM-TTCTGACCTGAAGGCTCTGCGCG-BHQ-1-3'	170 nM
R2	5'-GATCGCGCCCCACTGCGTTCTCCATTCTGG-3'	250 nM

285

286

287 *Standard RT-PCR with purified RNA*

288 Reference Cq values were obtained using the Allplex 2019-nCoV Assay (Seegene, Seoul,  
 289 South Korea) according to the manufacturer's instructions. 8 µL of purified RNA were used  
 290 to run 25 µL reactions on a Bio-Rad CFX96 and analysed with Seegene Viewer Software  
 291 version 3.18.

292

293 *High temperature RT-PCR with purified RNA*

294 Throughout this study high-temperature RT-PCR on RNA purified from either the in vitro  
295 transcribed viral genome fragment or the swab material was performed with the  
296 Volcano3G RT-PCR Probe 2x Master Mix (in short: Volcano3G) (myPOLS Biotec,  
297 Konstanz, Germany) using the CDC-approved N1 primer/probe mix from Integrated DNA  
298 Technologies (IDT, San Diego, CA, USA). In addition, sequence-identical primers and  
299 probe were obtained from Microsynth AG (Balgach, Switzerland) to produce data  
300 presented in Supplemental Fig. S1. Typically, 10 µl reactions were set up containing 1 µl  
301 RNA, 1x Volcano3G MasterMix, CDC\_N1 or RNaseP primer/probe mix (see table 1) and  
302 250 nM R2 primer. A three-stage thermal cycling program was performed on a Roche  
303 LightCycler 96, consisting of 1) 150 seconds at 75°C, 2) 10 cycles of 95°C for 5 seconds,  
304 150 seconds at 75°C, 3) 45 cycles of 95°C for 10 seconds, 57°C for 35 seconds. All assays  
305 were performed in white low profile tubes with ultra-clear caps (ThermoFisher, Cat No:  
306 AB1771) as singleplex with FAM/BHQ1-labelled probes. Cq values were determined with  
307 Roche LightCycler Software 1.1.0.

308

309 *High temperature RT-PCR with unprocessed patient material*

310 Nasopharyngeal swabs were eluted in 350 µl RNase/DNase free deionized water. These  
311 unprocessed samples were added directly to the PCR reaction. Reaction conditions were  
312 identical to those described for purified RNA as template, with the exception that the  
313 reaction volume was increased to 50 µl and 12 µl unprocessed sample was used (unless  
314 otherwise stated in the results section). In addition, successful amplification could be

315 visualised by detection of the dequenched fluorescein signal (FAM) on a blue light  
316 transilluminator (Safe Imager 2.0, Invitrogen).

317

### 318 *Treatments for improving high-temperature RT-PCR of raw patient samples*

319 In an effort to improve the efficiency of our protocol on unprocessed patient samples,  
320 several treatment regimens were tested. Nasopharyngeal swab samples in distilled water  
321 were supplemented with 1 ng/ $\mu$ l carrier RNA (Jena Analytik), 100 mM betaine (molecular  
322 grade, Sigma Aldrich), 0.05% bovine serum albumin (BSA) or a combination of all three,  
323 before adding the samples directly to the Volcano3G master mix. In another approach,  
324 swab samples were treated with 128  $\mu$ g/ $\mu$ l nuclease-free proteinase K (Analytik Jena) for  
325 10 minutes at 70°C in 5 mM HEPES (pH 7.4) followed by inactivation for 10 minutes at  
326 95°C. Alternatively, samples were treated with 2.5 mM nuclease-free DTT (Thermo Fisher  
327 Scientific) for 10 minutes at 70°C or a combination of proteinase K and DTT.

328

### 329 *Limit of detection (LOD) analysis*

330 Serial dilutions of the in vitro transcribed amplicon were made in water containing 5 ng/ $\mu$ l  
331 RNA carrier mix (innuPREP Virus DNA/RNA Kit, Analytik Jena) and real-time PCR  
332 reactions (10  $\mu$ l reaction volume) were set up as described above. Three to eight replicate  
333 reactions were conducted containing  $1 \times 10^6$ ,  $1 \times 10^5$ ,  $1 \times 10^4$ ,  $1 \times 10^3$ , 100, 10, 5, 3 or 1 copies  
334 per reaction. To estimate the LOD, the fraction of positive reactions ( $C_q < 40$ ) was plotted  
335 against the log-transformed number of amplicon copies.

336

### 337 *Statistical analysis*

338 Linear regression analysis was performed with Prism (GraphPad, La Jolla, CA, USA).

339 **Acknowledgements**

340 We thank the members of the AG Hauck and AG Groettrup for their help in processing  
341 patient samples, Thomas Meyer and Silke Müller from the Screening Center of University  
342 of Konstanz for automated RNA isolation, and Susanne Feindler-Boeckh for expert  
343 technical assistance. TB acknowledges support from the Konstanz Research School  
344 Chemical Biology (KoRS-CB) and AM support by the German Research Foundation  
345 (DFG) within SPP 1784.

346

347 **Author contributions**

348 JK, TB: conceived and performed experiments, analysed data, prepared figures and  
349 drafted the manuscript; MK, JZ: analysed samples and data, commented on the  
350 manuscript; LI, MS: recruited patients, procured samples, commented on the manuscript;  
351 RK, AM: provided essential reagents, consulted on experiments and commented on the  
352 manuscript; CRH: conceived the study, analysed data, wrote the manuscript.

353

354

355 **Conflict of interest**

356 AM, RK are founders of and employed by myPOLs Biotec GmbH, manufacturer of  
357 Volcano3G polymerase used in this manuscript.

358 All other authors declare that they have no conflict of interest.

359

360

361 **References**

- 362 Blatter N, Bergen K, Nolte O, Welte W, Diederichs K, Mayer J, Wieland M, Marx A (2013)  
363 Structure and function of an RNA-reading thermostable DNA polymerase. *Angew*  
364 *Chem Int Ed Engl* 52: 11935-9
- 365 Brierley I, Digard P, Inglis SC (1989) Characterization of an efficient coronavirus ribosomal  
366 frameshifting signal: requirement for an RNA pseudoknot. *Cell* 57: 537-47
- 367 Corman VM, Landt O, Kaiser M, Molenkamp R, Meijer A, Chu DK, Bleicker T, Brunink S,  
368 Schneider J, Schmidt ML, Mulders DG, Haagmans BL, van der Veer B, van den Brink  
369 S, Wijsman L, Goderski G, Romette JL, Ellis J, Zambon M, Peiris M et al. (2020)  
370 Detection of 2019 novel coronavirus (2019-nCoV) by real-time RT-PCR. *Euro Surveill*  
371 25: pii=2000045
- 372 Den Boon JA, Spaan WJ, Snijder EJ (1995) Equine arteritis virus subgenomic RNA  
373 transcription: UV inactivation and translation inhibition studies. *Virology* 213: 364-72
- 374 Irigoyen N, Firth AE, Jones JD, Chung BY, Siddell SG, Brierley I (2016) High-Resolution  
375 Analysis of Coronavirus Gene Expression by RNA Sequencing and Ribosome Profiling.  
376 *PLoS Pathogens* 12: e1005473
- 377 Lescure FX, Bouadma L, Nguyen D, Parisey M, Wicky PH, Behillil S, Gaymard A,  
378 Bouscambert-Duchamp M, Donati F, Le Hingrat Q, Enouf V, Houhou-Fidouh N, Valette  
379 M, Mailles A, Lucet JC, Mentre F, Duval X, Descamps D, Malvy D, Timsit JF et al.  
380 (2020) Clinical and virological data of the first cases of COVID-19 in Europe: a case  
381 series. *The Lancet Infectious Diseases* doi: 10.1016/S1473-3099(20)30200-0. [Epub  
382 ahead of print]
- 383 Lu R, Zhao X, Li J, Niu P, Yang B, Wu H, Wang W, Song H, Huang B, Zhu N, Bi Y, Ma X,  
384 Zhan F, Wang L, Hu T, Zhou H, Hu Z, Zhou W, Zhao L, Chen J et al. (2020) Genomic  
385 characterisation and epidemiology of 2019 novel coronavirus: implications for virus  
386 origins and receptor binding. *Lancet* 395: 565-574
- 387 Nedialkova DD, Gorbalenya AE, Snijder EJ (2010) Arterivirus Nsp1 modulates the  
388 accumulation of minus-strand templates to control the relative abundance of viral  
389 mRNAs. *PLoS Pathogens* 6: e1000772

- 390 Pan Y, Zhang D, Yang P, Poon LLM, Wang Q (2020) Viral load of SARS-CoV-2 in clinical  
391 samples. *The Lancet Infectious Diseases* 20: 411-412
- 392 Plant EP, Perez-Alvarado GC, Jacobs JL, Mukhopadhyay B, Hennig M, Dinman JD (2005)  
393 A three-stemmed mRNA pseudoknot in the SARS coronavirus frameshift signal. *PLoS*  
394 *Biology* 3: e172
- 395 Sauter KB, Marx A (2006) Evolving thermostable reverse transcriptase activity in a DNA  
396 polymerase scaffold. *Angew Chem Int Ed Engl* 45: 7633-5
- 397 Snijder EJ, Decroly E, Ziebuhr J (2016) The Nonstructural Proteins Directing Coronavirus  
398 RNA Synthesis and Processing. *Advances in Virus Research* 96: 59-126
- 399 Wu F, Zhao S, Yu B, Chen YM, Wang W, Song ZG, Hu Y, Tao ZW, Tian JH, Pei YY, Yuan  
400 ML, Zhang YL, Dai FH, Liu Y, Wang QM, Zheng JJ, Xu L, Holmes EC, Zhang YZ (2020)  
401 A new coronavirus associated with human respiratory disease in China. *Nature* 579:  
402 265-269
- 403 Zhou P, Yang XL, Wang XG, Hu B, Zhang L, Zhang W, Si HR, Zhu Y, Li B, Huang CL,  
404 Chen HD, Chen J, Luo Y, Guo H, Jiang RD, Liu MQ, Chen Y, Shen XR, Wang X, Zheng  
405 XS et al. (2020) A pneumonia outbreak associated with a new coronavirus of probable  
406 bat origin. *Nature* 579: 270-273
- 407 Zou L, Ruan F, Huang M, Liang L, Huang H, Hong Z, Yu J, Kang M, Song Y, Xia J, Guo  
408 Q, Song T, He J, Yen HL, Peiris M, Wu J (2020) SARS-CoV-2 Viral Load in Upper  
409 Respiratory Specimens of Infected Patients. *New England Journal of Medicine* 382:  
410 1177-1179
- 411 Zumla A, Al-Tawfiq JA, Enne VI, Kidd M, Drosten C, Breuer J, Muller MA, Hui D, Maeurer  
412 M, Bates M, Mwaba P, Al-Hakeem R, Gray G, Gautret P, Al-Rabeeah AA, Memish ZA,  
413 Gant V (2014) Rapid point of care diagnostic tests for viral and bacterial respiratory  
414 tract infections--needs, advances, and future prospects. *The Lancet Infectious*  
415 *Diseases* 14: 1123-1135
- 416

417 **Figure legends**

418

419 **Figure 1. A RNA- and DNA-reading heat-stable polymerase reverse transcribes and**  
420 **amplifies viral RNA. A)** Schematic overview of the SARS-CoV-2 genome. The target  
421 sequences for the N1 primers and probe are marked in red and green, respectively. The  
422 R2 primer binding sequence is underlined. Sequences divergence between SARS-CoV-  
423 2 and SARS-CoV-1 genomes are highlighted in blue. **B)** Performance of Volcano3G  
424 polymerase was compared to Taq polymerase using plasmid DNA or in vitro transcribed  
425 RNA as template (5000 viral genome equivalents). **C)** Determination of the linear dynamic  
426 range for the Volcano3G protocol with or without an additional primer (R2) for optimized  
427 reverse transcription at a final concentration of 250 nM. In vitro transcribed RNA  
428 containing the Sars-CoV-2 N amplicon was serially diluted in the range from  $1 \times 10^6$  copies  
429 to 10 copies. **D)** Limit of detection (LOD) was assessed with serial dilutions ranging from  
430 20 to 1 copy per reaction ( $n=6$  for each dilution). The fraction of positive reactions (y-axis)  
431 were plotted against the log-transformed number of RNA copies per reaction. Addition of  
432 R2 primer enhances the performance at lower copy-numbers. **E)** Amplification curves  
433 showing the performance of Volcano3G on isolated RNA from two COVID-19 patients in  
434 presence or absence of R2.

435

436 **Figure 2. SARS-CoV-2 detection by high-temperature RT-PCR in a patient cohort**  
437 **delivers results consistent with the standard procedure. A)** RNA was isolated from  
438 nasopharyngeal- and throat swab samples ( $n= 43$ ) and SARS-CoV-2 and RNaseP were  
439 detected using the Volcano3G protocol. N1 amplicon (blue), RNaseP gene (gray). Water  
440 was used as a non-template control (light gray). **B)** Identical samples were processed in  
441 parallel in an accredited diagnostic lab using the Allplex 2019-nCoV assay from Seegene.  
442 Direct comparison of assay results reveals 100% concordance of Volcano3G with the  
443 reference assay. **C)** Cq values obtained with Volcano3G were lower than those obtained  
444 with the reference assay ( $\Delta Cq = 6.4 \pm 0.78$ ). **D)** For each positive patient sample, the Cq  
445 values obtained with both assays were plotted against each other for linear regression  
446 analysis. A highly significant correlation of Volcano3G with the reference assay was  
447 observed ( $r^2=0.98$ ,  $p<0.0001$ ).

448

449 **Figure 3. High-temperature RT-PCR using Volcano3G polymerase allows SARS-**  
450 **CoV-2 detection from unprocessed patient samples** **A)** Nasopharyngeal- and throat  
451 swab samples (prepared in water) were added directly as template for RT-qPCR using  
452 the Volcano3G protocol. Representative amplification curves of patients with high (dark  
453 blue), medium (medium blue) and low Cq as well as negative patients (light blue) are  
454 shown. **B)** RNA was isolated from the remaining patient material and analysed in an  
455 accredited diagnostic lab using the Allplex 2019-nCoV assay from Seegene. **C)** The Cq  
456 values of each patient sample are compared between the reference protocol and the  
457 Volcano3G direct approach. Dotted red line indicates the cut-off, where the assay loses  
458 sensitivity. **D)** For each positive patient sample, the Cq values obtained with both assays  
459 were plotted against each other for linear regression analysis ( $r^2=0.779$ ,  $p<0.0001$ ) **E)** RT-  
460 PCR analysis of 100 copies of in vitro transcribed RNA spiked with varying amounts of  
461 pooled patient material from 5 confirmed negative patients. **F)** RT-PCR analysis of  
462 confirmed COVID-19 patient samples with high Cq values were analysed in a larger  
463 volume. **G)** Four confirmed COVID-19 patient samples and one negative control were  
464 used directly as in A). The reference cq-values obtained by standard RT-PCR from  
465 purified RNA (upper row) and the cq-values obtained by high temperature RT-PCR with  
466 Volcano3G polymerase (lower row) are given. After completion of PCR cycling, the reaction  
467 tubes were photographed on a blue light transilluminator (470 nm). Positive samples  
468 emitted a distinct green fluorescence visible by the naked eye.

469

470 **Supplementary Figure S1. The R2 reverse primer enhances detection of the viral N**  
471 **gene RNA.** **A)** N1 oligonucleotides and fluorescent probes according to CDC's  
472 recommendations were ordered from an alternative manufacturer (Microsynth AG) and  
473 assessed for their performance using Volcano3G and 500 copies of in vitro transcribed  
474 RNA encoding the N1 amplicon. Concentration of forward and reverse primers were  
475 adjusted for optimal performance. **B)** The chosen primer/probe concentrations were  
476 evaluated using isolated RNA from two confirmed SARS-CoV-2 positive patients, using  
477 RNaseP as control (dashed grey lines). Dashed blue lines: primer/probe pair without R2.  
478 Addition of R2 reverse primer at a final concentration of 250 nM enhanced the  
479 performance of the N1 primer pair, while showing no effect on RNaseP amplification (solid

480 blue and grey lines, respectively). Light grey line: non-template control. **C)** Amino acid  
481 sequences of the amino-terminus of the beta-coronavirus N gene from SARS-CoV-2,  
482 SARS-CoV-1, MERS, and the human coronavirus strains OC43, HKU1, 229E, and NL63.  
483 Identical amino acids are marked in red. The N protein displays high sequence divergence  
484 at the amino terminus suggesting that the corresponding region of the N gene (upper row)  
485 is well suited for selective detection of SARS-CoV-2. **D)** Isolated RNA from a confirmed  
486 SARS-CoV-2 positive patient was analysed using the Volcano3G protocol and the N1  
487 primer/probe mix from IDT in presence of 250 nM of R2. A temperature gradient was run  
488 during the reverse transcription reaction (step 1 and 2) of the Volcano3G thermocycling  
489 program.

490  
491 **Supplementary Figure S2. Swab-derived material contains inhibitory factors. A)**  
492 Nasopharyngeal swab samples from three confirmed negative patients were serially  
493 diluted in RNase free water and spiked with 5000 copies of in vitro transcribed RNA  
494 revealing the presence of PCR inhibitors. **B)** Unprocessed patient material from two  
495 confirmed SARS-CoV2 positive patients and isolated RNA from one confirmed positive  
496 patient were serially diluted in RNase free water containing carrier RNA (1 ng/ $\mu$ l).  
497 Empirically determined Cq values are plotted against a theoretical dilution curve.

498  
499 **Supplementary Figure S3. The inhibitory effects of raw patient material can be**  
500 **ameliorated. A)** An unprocessed nasopharyngeal swab sample of a confirmed SARS-  
501 CoV-2 positive patient was diluted in water plus either carrier RNA (1ng/ $\mu$ l), betaine (100  
502 mM), BSA (0.05%) or a combination of all three and subjected to Volcano RT-qPCR. **B)**  
503 Nasopharyngeal swab sample of a confirmed positive patient was diluted in water plus  
504 carrier RNA (1 ng/ $\mu$ l). Patient material was then treated with Proteinase K (ProtK, 128  
505  $\mu$ g/ml), DTT (2.5 mM) or a combination of both. Samples were incubated at 70°C for 10  
506 min. Samples containing ProtK were additionally inactivated at 95°C for 10 min.

**Figure 1**

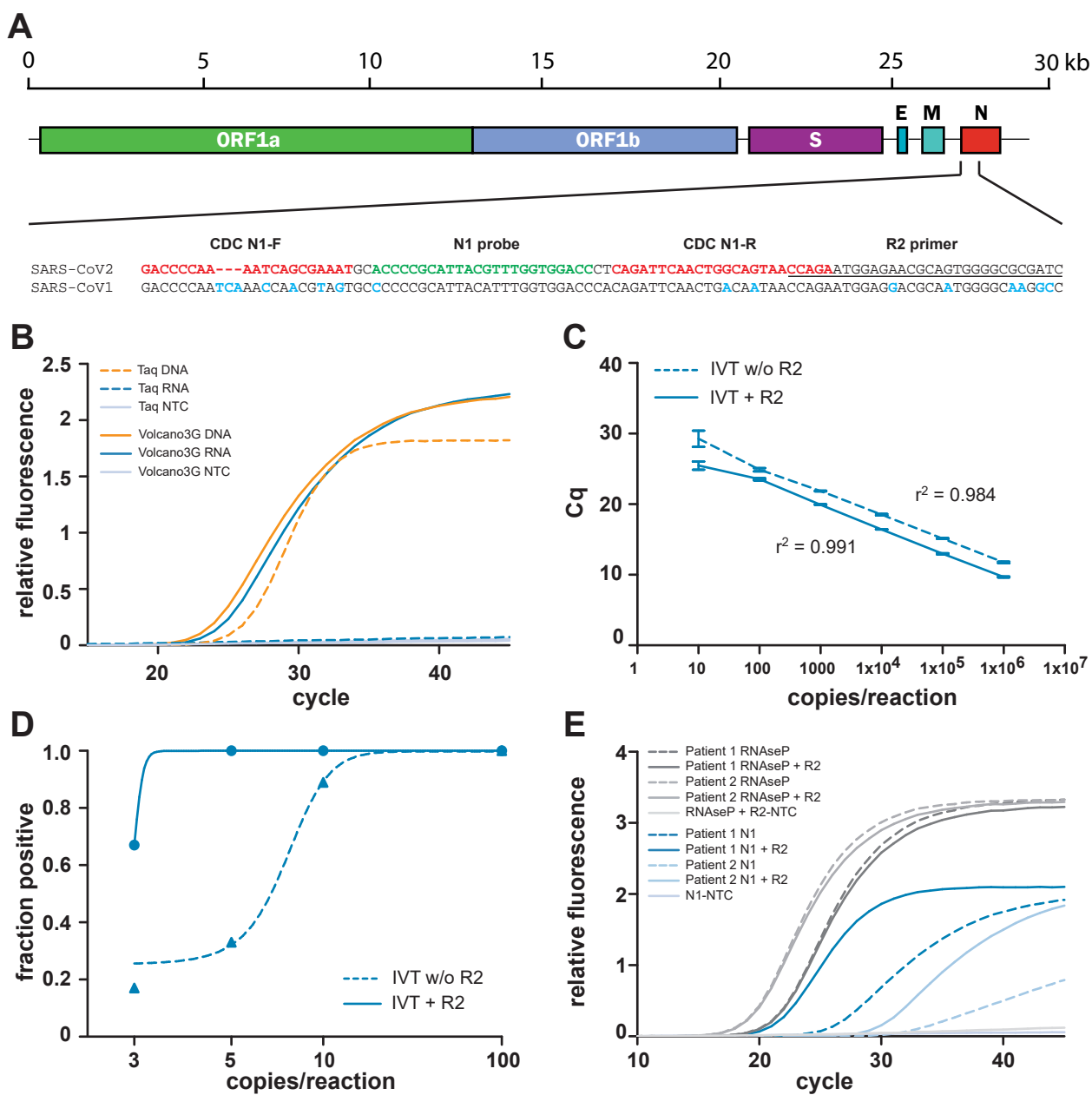
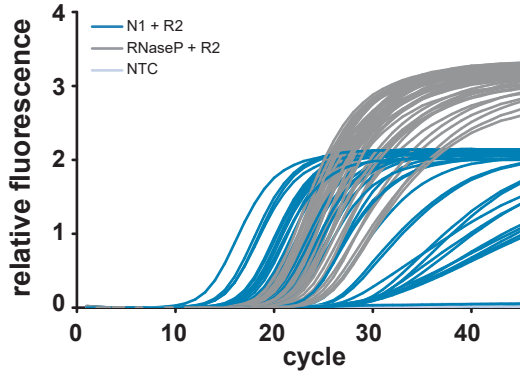


## Figure 2

**A**

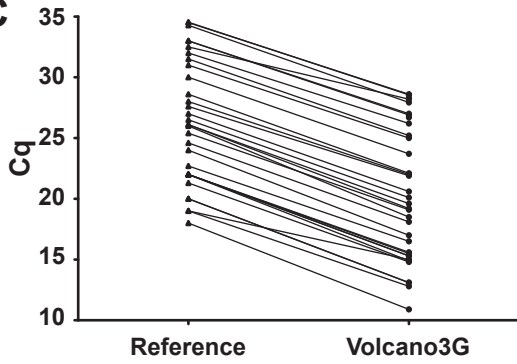


**B**

		Volcano3G	
		positive	negative
Reference	positive	35	0
	negative	0	8

Sensitivity: 100%    False positive rate: 0%  
Specificity: 100%    False negative rate: 0%

**C**



**D**

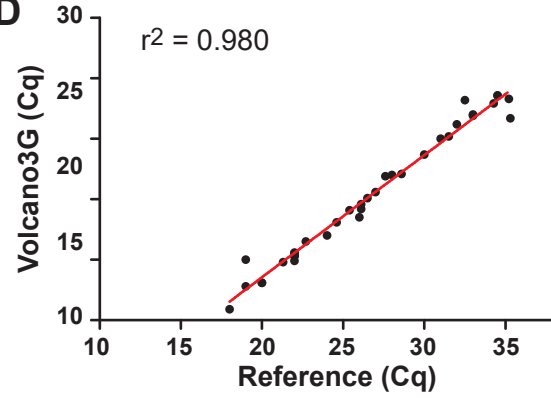
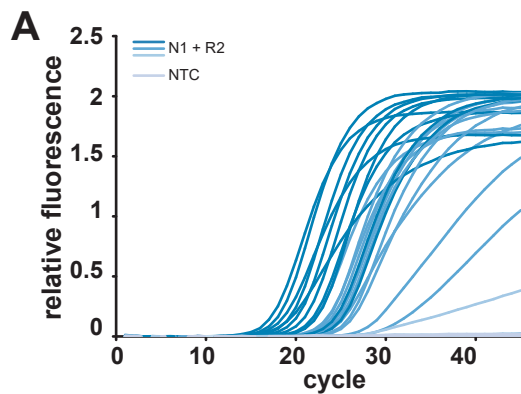
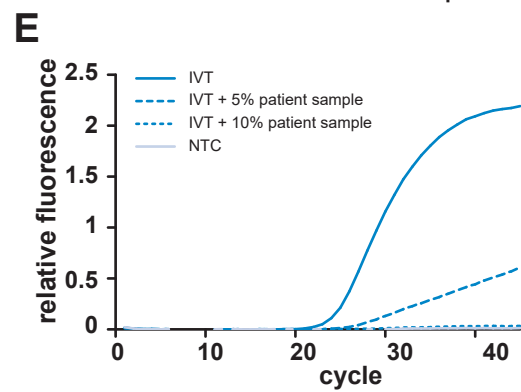
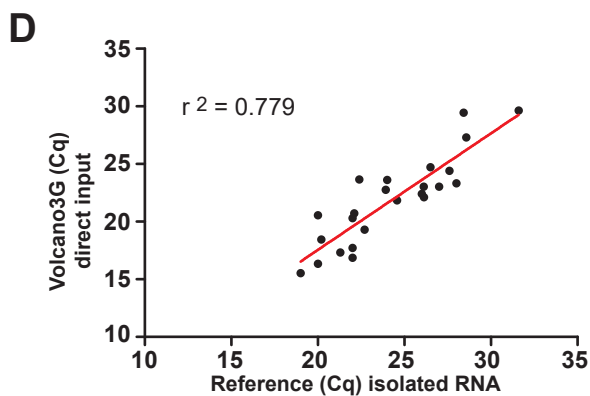
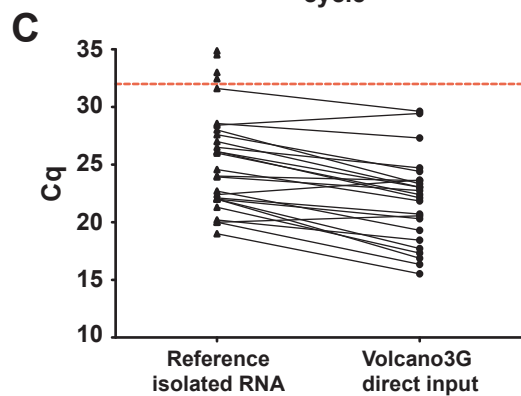


### Figure 3



**B**

		Volcano3G							
		Cq < 24		Cq 24-30		Cq > 30		negative	
Reference	positive	12	0	12	0	1	4	0	0
	negative	0	0	0	0	0	0	0	12
false positive:		0%		0%		0%		0%	
false negative:		0%		0%		80%		0%	



**F**

Sample	Reference Cq	Volcano3G Cq
1	34.3	32.18
2	28.01	25.89
3	35.2	-
4	34.5	30.8
5	35.3	-
6	32.0	31.26
7	31.5	-

